

Molecular-field approach to the spin-Peierls transition in CuGeO₃

Ralph Werner and Claudius Gros

Universität Dortmund, Institut für Physik, D-44221 Dortmund, Germany

(July 11, 2021)

We present a theory for the spin-Peierls transition in CuGeO₃. We map the elementary excitations of the dimerized chain (solitons) on an effective Ising model. Inter-chain coupling (or phonons) then introduces a linear binding potential between a pair of soliton and anti-soliton, leading to a finite transition temperature. We evaluate, as a function of temperature, the order parameter, the singlet-triplet gap, the specific heat, and the susceptibility and compare with experimental data on CuGeO₃. We find that CuGeO₃ is close to a first-order phase transition. We point out, that the famous scaling law $\sim \delta^{2/3}$ of the triplet gap is a simple consequence of the linear binding potential between pairs of solitons and anti-solitons in dimerized spin chains.

I. INTRODUCTION

With the discovery of the first inorganic spin-Peierls compound CuGeO₃¹ it has become possible to investigate the physics of the spin-Peierls transition in quasi one-dimensional spin chains with high precision. Of particular interest has been the study of the magnetic excitation spectrum by neutron scattering²⁻⁴ and Raman scattering experiments^{5,6}. It has been observed^{4,7}, that the spin-Peierls gap, i.e. the gap to triplet excitations out of the singlet ground-state, has a temperature dependence which is difficult to explain with existing theories of the spin-Peierls transition^{8,9}.

Existing theories of the spin-Peierls transition of spin-1/2 Heisenberg chains are based on the mapping of the spin chain to an interacting gas of spin-less fermions via the Jordan-Wigner transformation^{8,9}. The chains are coupled to a three-dimensional phonon mode and the transition occurs when the respective phonon frequency becomes soft. In the spin-Peierls state the unit-cell doubles due to the alternating displacements of the magnetic ions. The effective Hamiltonian for the magnetic excitations along the chains in the dimerized state is then¹⁰

$$H = J \sum_i [(1 + \delta(-1)^i) \mathbf{S}_i \cdot \mathbf{S}_{i+1} + \alpha \mathbf{S}_i \cdot \mathbf{S}_{i+2}]. \quad (1)$$

The nearest neighbor (NN) exchange has alternating strength $J(1 \pm \delta)$ due to the doubling of the unit cell below the spin-Peierls transition temperature T_{SP} . Also included in (1) is a frustrating next-nearest-neighbor (NNN) term $\sim J\alpha$. The ground-state phase diagram of (1) has been mapped out by a density matrix renormalization group study¹¹. There is a gap everywhere in the

phase-diagram except on the line $\delta = 0$ and $\alpha < \alpha_c$, with $\alpha_c \approx 0.2411$. A vividly debated question of key interest is therefore the actual magnitude of the strength of the frustration α . For CuGeO₃ the parameters have been estimated as $J \approx 150-160\text{K}$ and $\alpha \approx 0.24-0.35$ ^{10,12,13}.

A consequence of existing theories of the spin-Peierls transition is the occurrence of a soft phonon mode above T_{SP} , which has not yet been observed for CuGeO₃¹⁴. It is therefore of interest to pursue the possibility of a purely electronically driven spin-Peierls transition, as it could occur for $\alpha > \alpha_c$. In such a scenario the phonons would just follow the pre-formed electronic dimerization, i.e. the formation of NN singlet pairs. Here we propose a simple molecular-field type theory for the spin-Peierls transition by mapping the low-energy solitonic excitations of dimerized spin chains on an effective Ising model. We emphasize that this procedure is valid both for the phonon-driven and for the electronically-driven spin-Peierls transition. We present results of the mean-field theory in comparison with experiments on CuGeO₃. We find that a straightforward determination of the frustration parameter α is not conclusive and that CuGeO₃ is close to a first-order phase transition. We also note that the famous $\sim \delta^{2/3}$ scaling of the triplet gap^{9,11} is a simple consequence of the linear binding potential between solitons and anti-solitons in dimerized spin chains.

II. MAPPING ON AN EFFECTIVE ISING MODEL

A strictly one-dimensional system shows no long-range order at finite temperatures due to the solitonic excitations. The appropriate solitons in a spin-Peierls state are domain-walls in between two different dimer coverings, see Fig. 1. In this picture a dimer consists of a NN pair of spins in singlet state. A single soliton in an otherwise (dimer-) ordered chain is in reality a complicated object¹⁵. It is spatially extended¹⁶ and has a spin degree of freedom together with a dispersion, which in the Majumdar-Gosh model ($\alpha = 1/2$ ¹⁷) has the form $J(5/4 - \cos 2k)$. It has been shown¹⁵, that the solitons yield an accurate description of the magnetic susceptibility and hence of the Hilbert space.

The dispersion of the solitons might be approximated, in general, by

$$E(k) = \sqrt{(E_s)^2 + (cJ \sin k)^2}, \quad (2)$$

where E_s is the gap to solitonic excitations, J the exchange integral, c a constant of order of unity, and

k is the wavenumber in units of inverse lattice spacings. Only the low-energy solitons are effective in destroying the long-range dimer order, and we approximate here (2) by a constant $E(k) \equiv E_s$. We will furthermore not discuss the consequence of the spatial extent of the solitons and we will include their spin-degree of freedom only when determining the susceptibility. We take one of the two possible dimer configurations of the linear chain as the reference state and label every “good” dimer by $+1$ and every bond between two “wrong” dimers by -1 ; A bond between a soliton and a wrong dimer is also labeled -1 as shown in Fig. 1. Every possible soliton configuration is therefore mapped to a Ising-spin configuration living on every second bond. A similar mapping has been used recently by Mostovoy and Khomskii¹⁸.

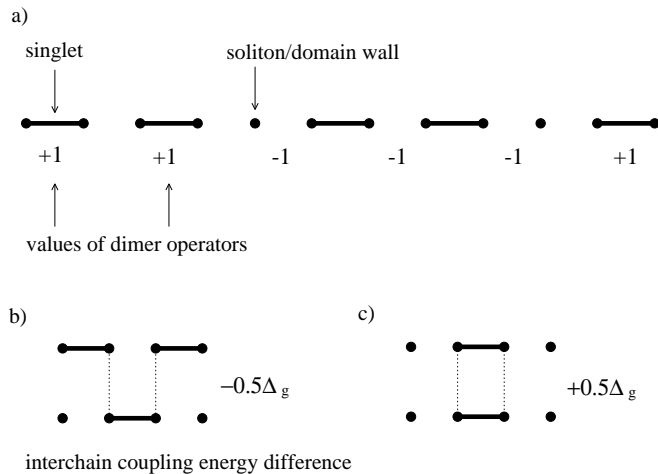


FIG. 1. *Phenomenological picture of copper chains in CuGeO₃.* a): A soliton and an anti-soliton in a dimerized chain with the corresponding values of the dimer operators $\sigma_{i,l}$. There is one dimer operator for every pair of sites. b) and c): Illustration of two different dimer configurations which lead to an inter-chain coupling contribution to the energy of $\pm 0.5\Delta_g$. The origin of the coupling may be attributed to the inter-chain exchange as well as to phononic effects.

We now consider a two-dimensional array of chains and define by $\sigma_{i,l} = \pm 1$ the Ising variable on the l^{th} chain, where the site index i runs over every second bond of a chain of length L . Including a coupling Δ_g between dimers on NN chains we have

$$H_{2D} = E_s \sum_{i,l} \frac{1}{2} (1 - \sigma_{i,l} \sigma_{i+1,l}) - \frac{\Delta_g}{2} \sum_{i,l} \sigma_{i,l} \sigma_{i,l+1} \quad (3)$$

as the effective Ising Hamiltonian. The inter-chain coupling Δ_g might be induced by the inter-chain exchange coupling, $J_{\perp} \approx 0.1J$. In this case $\Delta_g \sim (J_{\perp})^2/J$. An indirect coupling of the chains via phonons is also conceivable⁸. It has been shown recently, that a molecular-field decoupling of inter-chain interactions in quasi one-dimensional systems is a good approximation

in the strongly anisotropic limit¹⁹. We may therefore decouple the chains via

$$\sigma_{i,l} \sigma_{i,l+1} \rightarrow \sigma_{i,l} \langle \sigma_{i,l+1} \rangle + \sigma_{i,l+1} \langle \sigma_{i,l} \rangle - \langle \sigma_{i,l} \rangle \langle \sigma_{i,l+1} \rangle, \quad (4)$$

where the $\langle \sigma_{i,l} \rangle$ denotes the thermodynamic expectation value. Translational invariance perpendicular to the chains yields $\langle \sigma_{i,l+1} \rangle = \langle \sigma_{i,l} \rangle = \langle \sigma \rangle$ and the Hamiltonian for a single chain (the number of Ising variables is $L/2$) becomes in this mean-field approximation

$$H = -\frac{1}{2} E_s \sum_{i=1}^{L/2} \sigma_i \sigma_{i+1} - B \sum_{i=1}^{L/2} \sigma_i + \frac{L}{4} E_s + \frac{L}{4} \Delta_g \langle \sigma \rangle^2, \quad (5)$$

where we have set $B = \Delta_g \langle \sigma \rangle$. This is just the Ising Hamiltonian for a ferromagnetic spin chain in an external magnetic field B . Alternatively we can interpret (5) as an effective model for domain walls in a spin-Peierls state with a linear binding potential $V(x) = B \cdot (x+1)$ (with $x \geq 1$ being the distance in sites, not bonds) between a soliton and an anti-soliton.

So far we have neglected the spin-phonon coupling λ_{sp} . A finite value for the spin-singlet order parameter $\langle \sigma \rangle$ leads through λ_{sp} to a finite lattice dimerization and consequently to a modulation of the exchange constant, $J(1 \pm \delta)$, in (1), with $\delta \sim \lambda_{sp} \langle \sigma \rangle$. The spin-phonon coupling therefore adds a term $\sim \lambda_{sp} \langle \sigma \rangle$ to the confining potential B . On a mean-field level this corresponds to a rescaling of the coupling constant

$$\Delta_g \rightarrow \Delta_g + c_1 \lambda_{sp}, \quad B \rightarrow B + c_2 \delta, \quad (6)$$

with appropriate constants c_1 and c_2 .

The partition function Z can be obtained from (5) by the transfer matrix method. The free energy $F = -k_B T \ln Z$ is given in the thermodynamic limit ($L \rightarrow \infty$) by

$$\frac{F}{L/2} = -k_B T \ln \lambda_0 + \frac{1}{2} \Delta_g \langle \sigma \rangle^2 \quad (7)$$

where

$$\lambda_0 = \cosh(\beta \Delta_g \langle \sigma \rangle) + \sqrt{\sinh^2(\beta \Delta_g \langle \sigma \rangle) + e^{-2\beta E_s}} \quad (8)$$

with $\beta = 1/(k_B T)$ being the inverse temperature. From the free energy all physical quantities can be derived.

III. EXCITATION ENERGIES

We have two relevant excitation energies, the gap to single soliton excitations, given by E_s in (5), and the gap to triplet excitations, Δ_N , as measured in a neutron scattering experiment⁴. Let us now discuss the relation of Δ_N to E_s .

A triplet excitation can dissolve into a soliton/anti-soliton pair. The linear binding energy $V(x) = B \cdot (x+1)$ in between a soliton and an anti-soliton in (5) leads to a confinement of soliton/anti-soliton pairs²⁰. In (5) we have neglected the kinetic energy of the single solitons (2), which is of order J . The energy levels of a particle in a linear confining potential are well known^{21,22}. The lowest eigenstate has, in the limit $B \ll J$, the energy

$$\Delta_N = 2E_s + c'J \left(\frac{B}{J}\right)^{2/3}, \quad (9)$$

with $c' \approx 2.33$. Eq. (9) gives then the gap to triplet excitations as a function of soliton energy E_s and the strength of the confining potential B . The mean extension of a soliton/anti-soliton pair scales like $(B/J)^{-1/3}$.

For $\alpha < \alpha_c$ we have $B \rightarrow c_2\delta$ and Eq. (9) takes then the form

$$\Delta_N \Big|_{\alpha < \alpha_c} \approx 2E_s + 2.33 v_s \left(\frac{c_2\delta}{v_s}\right)^{2/3}, \quad (10)$$

where $v_s \approx (\pi/2)(1 - 1.12\alpha)J$ is the α -dependent spin-wave velocity²³. It is known^{9,11}, that the gap scales for $\alpha < \alpha_c$ like $\sim \delta^{2/3}$ implying that $E_s\delta^{-2/3} \rightarrow 0$ for $\delta \rightarrow 0$. Comparison with numerical results¹¹ leads to $c_2 \approx 0.85$. The functional form of the dependence of the soliton excitation energy E_s on δ , or alternatively on the dimerization order parameter $\langle\sigma\rangle$ is not known at present. It might be extracted for $\alpha < \alpha_c$, in principle, from a sub-leading scaling analysis of the excitation energy

$$\Delta_N = \tilde{c}J(\delta)^{2/3} + 2E_s(\delta), \quad (11)$$

but this has not yet been done. We have therefore decided to assume the functional form

$$E_s(\langle\sigma\rangle) = E_\infty + (E_0 - E_\infty)\langle\sigma\rangle^2, \quad (12)$$

where E_0 is the zero-temperature value of E_s and where E_∞ is the soliton energy in the disordered phase, i.e. for $T > T_{SP}$. Eq. (12) is, in the spirit of a Landau functional (13), the simplest form consistent with the symmetry of $\langle\sigma\rangle$.

IV. LANDAU EXPANSION

We may expand the free energy (7) in powers of $\langle\sigma\rangle$,

$$F = F_0 + a(T)\langle\sigma\rangle^2 + b(T)\langle\sigma\rangle^4 + O(\langle\sigma\rangle^6). \quad (13)$$

Depending on the parameters we may have either a second-order phase transition with $b(T) > 0$ or a first-order phase transition with $b(T) < 0$. In the first case the transition temperature T_{SP} is given by $a(T_{SP}) = 0$ as

$$k_B T_{SP} = \frac{\Delta_g^2(1 + e^{-\beta E_\infty})}{2(E_0 - E_\infty)e^{-2\beta E_\infty} + \Delta_g(1 + e^{-\beta E_\infty})e^{-\beta E_\infty}}, \quad (14)$$

with $\beta \rightarrow 1/(k_B T_{SP})$. This transcendental equation takes a simple form in some limiting cases:

$$\begin{aligned} E_\infty = 0 : & \quad T_{SP} = \Delta_g^2/(\Delta_g + E_0) \\ E_\infty = E_0 : & \quad T_{SP} = \Delta_g e^{E_0/(k_B T_{SP})} \\ \Delta_g \rightarrow \infty : & \quad T_{SP} \rightarrow \Delta_g - E_0 + 2E_\infty \end{aligned} \quad (15)$$

For illustration we present in Fig. 2 (a) T_{SP} as a function of the inter-chain coupling constant Δ_g for $E_0 = 0.2\text{meV}$.

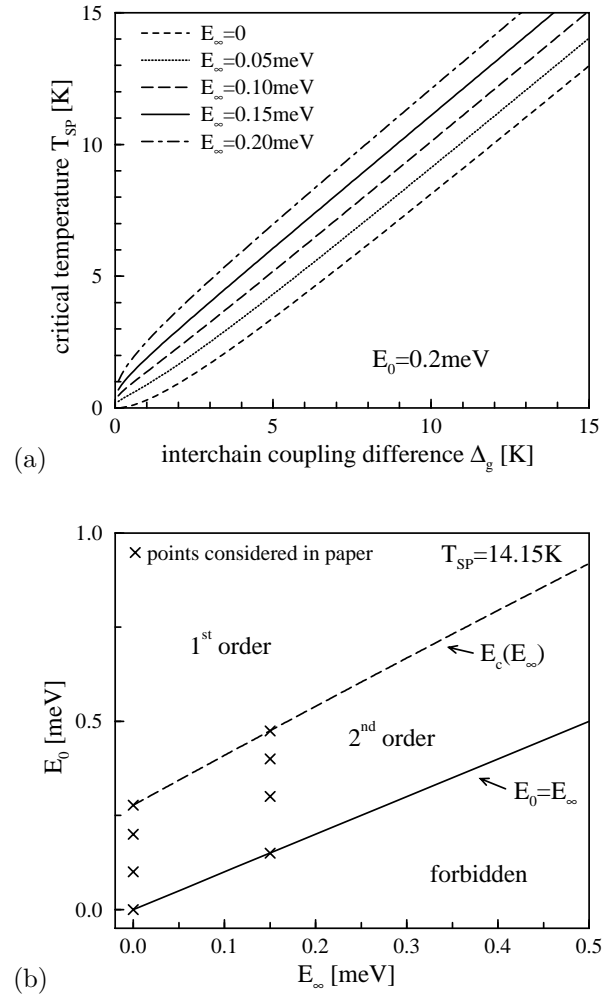


FIG. 2. (a): Illustration of the spin-Peierls transition temperature T_{SP} for $E_0 = 0.2\text{meV}$ as a function of Δ_g . (b): Phase diagram as a function of E_∞ and E_0 for fixed $T_{SP} = 14.15\text{K}$. Only the region $E_0 > E_\infty$ is allowed (above the solid line). Above the dashed line the phase transition is of first-order, below it is of second-order. The crosses indicate the parameter values considered for comparison with CuGeO_3 .

For $b(T_{SP}) < 0$ we obtain a first-order phase transition. This is the case for values of E_0 larger than a certain critical value of the soliton energy E_c , which is determined from $b(T_{SP}) = 0$ as

$$E_c = E_\infty + \frac{\Delta_g^2}{T_{SP}} \left(1 + e^{E_\infty/T_{SP}}\right)^2 \cdot \left(\sqrt{\frac{1 + 3e^{E_\infty/T_{SP}} + 3e^{2E_\infty/T_{SP}}}{6(1 + e^{E_\infty/T_{SP}})^2}} - \frac{1}{2} \right). \quad (16)$$

For a fixed transition temperature $T_{SP} = 14.15\text{K}$ and using Eq. (14), E_c and the corresponding inter-chain coupling energy Δ_g can be calculated as a function of E_∞ . The resulting phase diagram is given in Fig. 2(b). The numerical results presented throughout this paper are obtained within the second-order regime, indicated by the crosses in Fig. 2(b).

V. SELF-CONSISTENCY EQUATION

The effective Hamiltonian Eq. (5) contains three free parameters, namely E_∞ , E_0 and Δ_g . We examine two scenarios. The first is the case of $\alpha_c > \alpha$ with $E_\infty = 0$. The second is the case of $\alpha_c < \alpha \approx 0.35$ with $E_\infty = 0.15\text{meV}$ corresponding to a gap in the disordered phase of $2E_\infty = 0.3\text{meV}$ ¹¹. For each case we consider a range of E_0 (see Fig. 2(b)) within the second-order regime, $E_\infty \leq E_0 \leq E_c$,

$$E_\infty = 0 \text{ meV}; \quad E_0 = 0, 0.1, 0.2, 0.277 \text{ meV} \quad (17)$$

$$2E_\infty = 0.3 \text{ meV}; \quad E_0 = 0.15, 0.3, 0.4, 0.474 \text{ meV} \quad (18)$$

The largest value of E_0 for each E_∞ corresponds to $E_c(E_\infty)$, compare Fig. 2(b). The experimental transition temperature $T_{SP} = 14.15\text{K}$ of CuGeO_3 then determines the coupling constant Δ_g ²⁴.

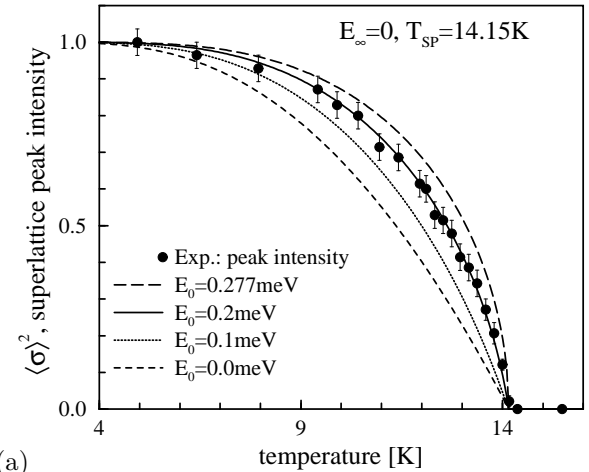
The order parameter $\langle \sigma \rangle$ is determined self-consistently as a function of temperature by setting the derivative of the free energy with respect to $\langle \sigma \rangle$ to zero,

$$\langle \sigma \rangle = \frac{\sinh(\beta \Delta_g \langle \sigma \rangle)}{2 \frac{E_0 - E_\infty}{\Delta_g \lambda_0} e^{-2\beta E_s} + \sqrt{\sinh^2(\beta \Delta_g \langle \sigma \rangle) + e^{-2\beta E_s}}}. \quad (19)$$

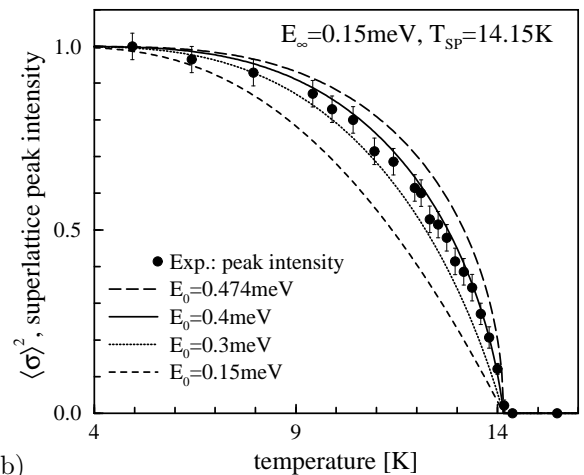
In Fig. 3 we show the results for $\sim \langle \sigma \rangle^2$ as a function of temperature for the parameters given in (17) and (18). We have also plotted the measured intensity of an additional super-lattice peak⁴, which is proportional to the square of the lattice dimerization. We have normalized the experimental data such that agreement is obtained in the low-temperature regime.

The comparison between theory and the data for CuGeO_3 does not lead to a determination of the frustration α but indicates closeness to a first-order phase

transition, as can be deduced from the closeness of the experimental points in Fig. 3 to the critical curves where $E_0 \approx E_c(E_\infty)$, compare Fig. 2(b).



(a)



(b)

FIG. 3. The square of the spin-singlet order parameter ($\langle \sigma \rangle^2$, lines) as a function of temperature, for two different values of E_∞ (soliton gap in the disordered phase) and several values of E_0 ($T = 0$ soliton gap). (a): $E_\infty = 0$, i.e. $E_s = E_0 \langle \sigma \rangle^2$. (b): $2E_\infty = 0.3\text{meV}$, i.e. $E_s = E_\infty + (E_0 - E_\infty) \langle \sigma \rangle^2$. For comparison we plot the measured⁴ intensity of an additional super-lattice peak (filled circles).

VI. THERMODYNAMICS

The entropy S and the specific heat c_V are obtained from the free energy (7) via

$$S = -\frac{\partial F}{\partial T}, \quad c_V = T \frac{\partial S}{\partial T}. \quad (20)$$

In the disordered phase the entropy is (for $E_\infty = 0$) temperature independent with a value of $k_B \ln(2)/2$ per site, which is only half of the expected value for a spin 1/2 chain. This is due to the fact that we did neglect up to now the spin-degrees of freedom of the domain-walls. In Fig. 4 we present results for $c_V(T)$ for the parameters given by (17) and (18).

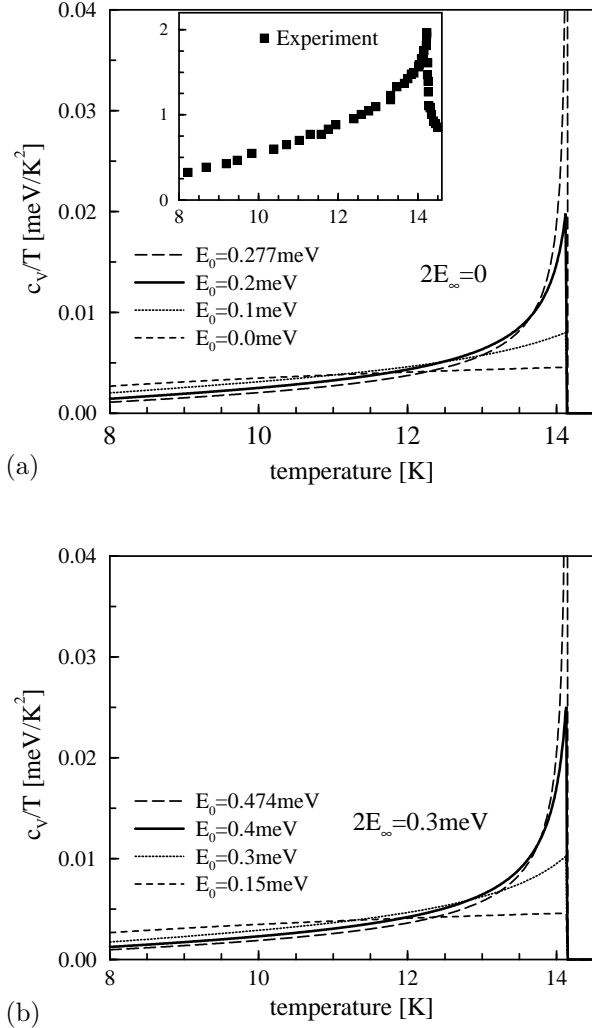


FIG. 4. Specific heat for different parameters as a function of temperature. (a): $E_\infty = 0$. (b): $2E_\infty = 0.3\text{meV}$. The inset in graph (a) shows the experimental data²⁵ of c_V/T in units of $[\text{mJ/gK}^2]$ versus T (10^{-2}meV/K^2 corresponds to 5.24mJ/gK^2).

For small soliton excitation energies the results are typically mean-field like. For values of E_0 approaching the limit of the second-order phase regime the specific heat is strongly enhanced near T_{SP} . It will diverge as the transition becomes first-order. Note that the specific heat is linear in temperature for $E_\infty \leq E_0 < E_c$, in the limit $T \rightarrow T_{SP}$ and that the jump in the specific heat diverges as $E_0 \rightarrow E_c$ like $(E_c - E_0)^{-1}$. Right at $E_0 = E_c$ the

specific heat diverges like $(T_{SP} - T)^{-1/2}$. Note that a similar divergence $\sim (T_{SP} - T)^{-0.4}$ has been reported in an early measurement for CuGeO_3 ²⁶ though the exact value of the specific heat critical exponent for CuGeO_3 is still controversial^{27,25}.

In the inset of Fig. 4 we present the measured magnetic contribution to the specific heat of CuGeO_3 ²⁵. A straightforward comparison with the results of the mean-field theory is not possible since all the entropy of the effective Ising chain is released in a mean-field approach. This corresponds to half of the entropy of the spin chain. Experimentally only $\sim 10\%$ of the magnetic entropy is released at T_{SP} ²⁸, since the exchange constant $J \approx 160\text{K} \gg T_{SP}$ and the measured specific heat is consequently smaller in magnitude than our mean-field result. The neglect of the soliton dispersion relation (2) is, on a microscopic level, the reason for this discrepancy between theory and experiment. A qualitative comparison is nevertheless possible and favors an E_0 close to the first-order phase transition.

Up to now we did not take the spin-degree of freedom of the solitons into account, as they just contribute a constant factor to the partition function in the paramagnetic case. As we have no magnetic interactions between the spins of different solitons in our model we can evaluate the magnetic susceptibility simply by Curie's law

$$\chi(T) = \frac{g^2 \mu_B^2 S(S+1)}{3k_B T} n(T) \approx 1.16 \frac{\mu_B^2}{k_B T} n(T), \quad (21)$$

where $\mu_B = e\hbar/(2m_e c)$ is the Bohr magneton, $g = 2.15$ the measured²⁹ g-factor of the Cu^{2+} -ion, $S = 1/2$ and $n(T)$ the density of thermally activated solitons per site. $n(T)$ is obtained differentiating the free energy with respect to E_s :

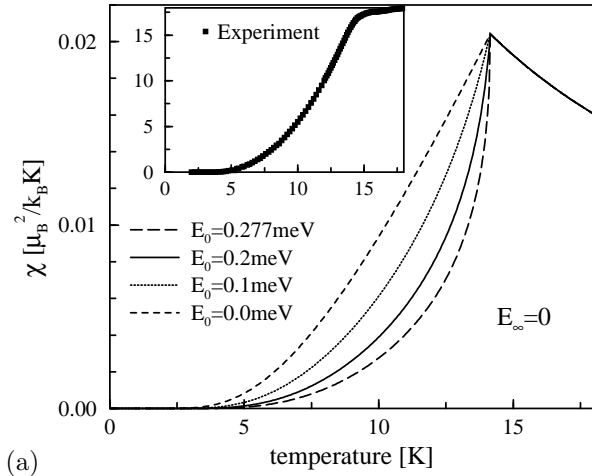
$$n(T) = \frac{\partial F/L}{\partial E_s} = \frac{1}{2\lambda_0} \frac{e^{-2\beta E_s}}{\sqrt{\sinh^2(\beta \Delta_g \langle \sigma \rangle) + e^{-2\beta E_s}}}. \quad (22)$$

Above T_{SP} this expression reduces to

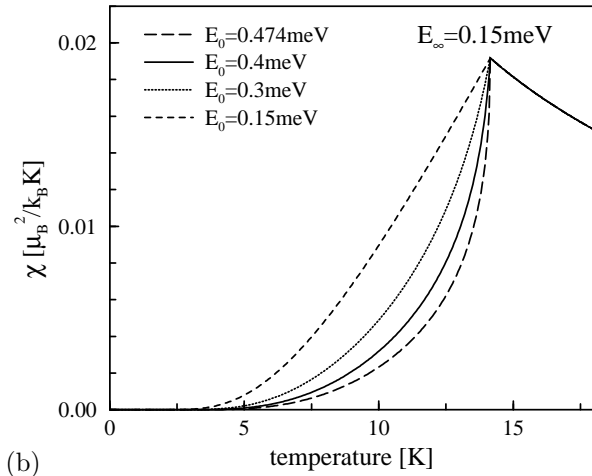
$$n(T > T_{SP}) = \frac{1}{2} \frac{1}{e^{\beta E_\infty} + 1}. \quad (23)$$

The mean number of solitons attains 1/4 per site, as the temperature goes to infinity, corresponding to half a soliton per dimer. The results for the magnetic susceptibility are shown in Fig. 5. The fast drop of $\chi(T)$ below T_{SP} for larger values of the soliton excitation energies is again reminiscent of the experimental data for CuGeO_3 ²⁹. Our susceptibility rises though much higher at T_{SP} than the experimental data which is a direct consequence of the neglected soliton dispersion (2). In the limit of large temperatures $T \gg J$ the theoretical curve drops to 1/4 of the experimental points as a consequence of the aforementioned soliton density (23) (at $300\text{K} \approx 2J$ it has dropped to about 1/2 of the magnitude of the experimental data).

Note that for the curves plotted as solid lines in Fig. 3, Fig. 4, and Fig. 5, which are closest to the experimental data within the parameters chosen by us, entropy, specific heat, and susceptibility are overestimated by about the same factor of five.



(a)



(b)

FIG. 5. Magnetic susceptibility for different parameters as a function of temperature. (a): $E_\infty = 0$. (b): $2E_\infty = 0.3\text{meV}$. The inset in graph (a) shows the experimental data²⁹ of χ in units of $[10^{-9}\text{m}^3/\text{mole}]$ versus T ($0.01\mu_B^2/k_B K$ correspond to $47.12 \cdot 10^{-9}\text{m}^3/\text{mole}$).

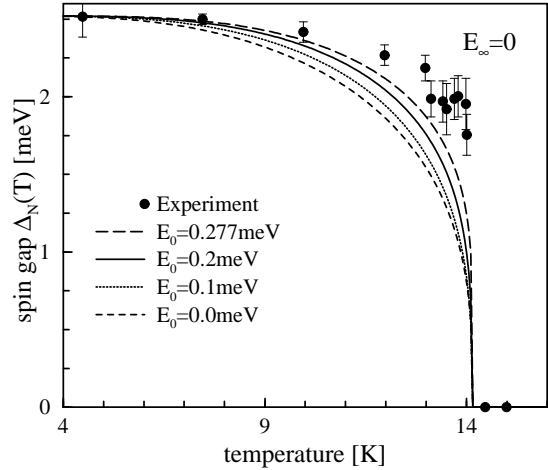
VII. SINGLET-TRIPLET GAP

The gap to triplet excitations is given by Eq. (9),

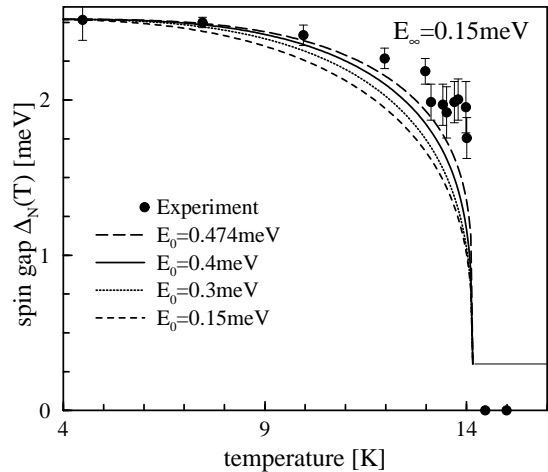
$$\Delta_N = 2(E_\infty + (E_0 - E_\infty)\langle\sigma\rangle^2) + c'J \left(\frac{\Delta_g\langle\sigma\rangle}{J} \right)^{2/3}, \quad (24)$$

with $c' = 2.33$. A straightforward application of (24) would yield, compared with experiment, a much too large

zero-temperature gap $2E_0 + c'J(\Delta_g/J)^{2/3}$. This is so since the order parameter $\langle\sigma\rangle(T=0)$ takes the value one in the molecular-field approximation, while it is much smaller than unity for CuGeO_3 . We have therefore decided to use the parameter c' in (24) to fix $\Delta_N(T=0)$ to the experimentally observed value 2.5meV . The results are given in Fig. 6, together with the measured gap for CuGeO_3 ⁴.



(a)



(b)

FIG. 6. The gap to triplet excitations for several parameters as a function of temperature. (a): $E_\infty = 0$. (b): $2E_\infty = 0.3\text{meV}$.

VIII. CONCLUSIONS

We have discussed a simple mean-field theory for spin-Peierls transitions applicable both for phonon-driven ($\alpha < \alpha_c$) and for magnetically driven ($\alpha > \alpha_c$) spin-Peierls transitions. We have applied the approach to CuGeO_3 and found that it is not possible to determine uniquely from the experimentally measured temperature

dependence of the order-parameter the magnitude of the frustration parameter α .

The theory allows both for a first-order and a second-order spin-Peierls transition, depending on the parameters of the model. We find that the parameters which fit experiments best indicate that CuGeO_3 is close to a first-order phase transition.

We would like to thank P. Lemmens and B. Büchner for discussions and J. Stolze for pointing out a straightforward derivation of the $\delta^{2/3}$ scaling law. The support of the DFG is gratefully acknowledged.

¹ M. Hase *et al.*, Phys. Rev. Lett. **70**, 3651 (1993).
² M. Nishi, O. Fujita, and J. Akimitsu, Phys. Rev. B **50**, 6508 (1994).
³ L.P. Regnault, M. Aïn, B. Hennion, G. Dhaleenne, and A. Revcolevschi, Phys. Rev. B, **53**, 5579 (1996).
⁴ M.C. Martin *et al.*, Phys. Rev. B **53**, R14 713 (1996).
⁵ P.H.M. van Loosdrecht *et al.*, Phys. Rev. Lett. **76**, 311 (1996).
⁶ V.N. Muthukumar, C. Gros, W. Wenzel, R. Valentí, P. Lemmens, B. Eisener, G. Güntherodt, M. Weiden, C. Geibel, and F. Steglich, Phys. Rev. B **54**, R9635 (1996).
⁷ J.G. Lussier, S.M. Coad, D.F. McMorrow, and D. McK. Paul, J. Phys.: Condens. Matt. **8**, L59 (1996).
⁸ E. Pytte, Phys. Rev. B **10**, 2039 and 4637 (1974).
⁹ M.C. Cross and D.S. Fisher, Phys. Rev. B **19**, 402 (1979).
¹⁰ G. Castilla, S. Chakravarty, and V.J. Emery, Phys. Rev. Lett. **75**, 1823 (1995).
¹¹ R. Chitra *et al.*, Phys. Rev. B **52**, 6581 (1995).
¹² K. Fabricius, A. Klümper, U. Löw, B. Büchner, and T. Lorenz, "Reexamination of the microscopic couplings of the quasi one-dimensional antiferromagnet CuGeO_3 ", Sissa-preprint cond-mat/9705036.
¹³ J. Riera and A. Dobry, Phys. Rev. B **51**, 16 098 (1995).
¹⁴ K. Hirota *et al.*, Phys. Rev. B **52**, 15412 (1995).
¹⁵ B. S. Shastry and B. Sutherland, Phys. Rev. Lett. **47**, 964 (1981).
¹⁶ V. Kiryukhin, B. Keimer, J.P. Hill, and A. Vigilante, Phys. Rev. Lett. **76**, 4608 (1996); J. Zang, S. Chakravarty and A.R. Bishop, Sissa-preprint cond-mat/9702185; A. Dobry and J.A. Riera, Sissa-preprint cond-mat/9704090.
¹⁷ C. K. Majumdar, J. Phys. C: Solid St. Phys. **3**, 911 (1970).
¹⁸ M. Mostovoy and D. I. Khomskii, to appear in Z. Physik B **41**, No.2 (1997); Sissa-preprint cond-mat/9703104.
¹⁹ K.M. Kojima *et al.*, Phys. Rev. Lett. **78**, 1787 (1997).
²⁰ D. I. Khomskii, W. Geertsma, and M. Mostovoy, Czech. Journ. of Physics v. **46**, Suppl. S6, 3239 (1996)
²¹ A change of variable $x \rightarrow B^{1/(2+\gamma)}x$ for the the stationary Schrödinger equation $-\Psi''(x) + B|x|^\gamma\Psi(x) = E\Psi(x)$ leads to $E \sim B^{2/(2+\gamma)}$. Here $\gamma = 1$.
²² L. N. Bulaevskii, É. L. Nagaev, and D. I. Khomskii, Sov. Phys. JETP **27**, 836 (1968)

²³ A. Fledderjohann and C. Gros, Europhys. Lett. **37**, 189 (1997).
²⁴ The complete sets of parameter values (E_0, E_∞, Δ_g) are in [meV]: (0,0,1.22), (0.1,0,1.31), (0.2,0,1.39), (0.277,0,1.45) for $\alpha < \alpha_c$ and (0.15,0.15,1.05), (0.3,0.15,1.2), (0.4,0.15,1.28), (0.474,0.15,1.33) for $\alpha > \alpha_c$.
²⁵ J.C. Lasjaunias *et al.*, Solid State Comm. **101**, 677 (1997).
²⁶ S. Sahling, J.C. Lasjaunias, P. Monceau, and A. Revcolevschi, Solid State Comm. **92**, 423 (1994).
²⁷ X. Liu, J. Wosnitza, H.v. Löhneysen, and R.K. Kremer, Z. Phys. B **98**, 163 (1995).
²⁸ M. Weiden *et al.*, Z. Phys. B **98**, 167 (1995).
²⁹ M. Weiden, unpublished; V. N. Muthukumar *et al.*, Phys. Rev. B **55**, 5944 (1997).